



Broadband HMSIW antenna using a demi hexagonal ring slot for X-band application

Dian Widi Astuti^{1*}, Muslim Muslim¹, Umairah Umairah¹, Huda A Majid², Syah Alam³,
Yusnita Rahayu⁴

¹Department of Electrical Engineering, Faculty of Engineering, Universitas Mercu Buana, Indonesia

²Department of Electrical Engineering, Faculty of Engineering Technology, Universiti Tun Hussein Onn Malaysia, Malaysia

³Department of Electrical Engineering, Faculty of Engineering, Universitas Trisakti, Indonesia

⁴Department of Electrical Engineering, Faculty of Engineering, Universitas Riau, Indonesia

Abstract

Microstrip antennas offer several advantages, including small size, easy fabrication, controllable polarity and radiation patterns, and easy integration with other components. These qualities make microstrip antennas more reliable than other antenna types. However, they also have limitations, such as lower radiation efficiency and narrow bandwidth, primarily due to the thin substrate thickness. Substrate integrated waveguide (SIW) is a type of microstrip antenna. SIW antennas come in two forms: one with a rectangular shape, typically designed as a slot, and the other in the form of a horn. However, SIW slot antennas face challenges with narrow impedance bandwidth due to the thin substrate, unlike conventional bulky hollow waveguides. The half-mode substrate integrated waveguide (HMSIW) slot antenna, which is a 50% miniaturized version of the SIW slot antenna, also suffers from reduced fractional bandwidth, resulting from the miniaturization and the thin substrate. This paper focuses on enhancing the bandwidth of HMSIW antennas by incorporating a demi-hexagonal ring slot. The broadband impedance bandwidth simulation (27.36%) is achieved through triple resonance frequencies to address the issue of narrow impedance bandwidth. Both the simulation results and measurements show consistency, with the measured impedance bandwidth ranging from 8.91 to 12.62 GHz (34.46%), demonstrating at least triple resonance frequencies.

This is an open access article under the [CC BY-SA](#) license



Keywords:

Bandwidth Enhancement;
Broadband Bandwidth;
Hexagonal slot;
HMSIW antenna;
Triple Resonance frequencies;

Article History:

Received: February 16, 2024

Revised: April 8, 2024

Accepted: April 18, 2024

Published: January 2, 2025

Corresponding Author:

Dian Widi Astuti

Electrical Engineering Department,
Faculty of Engineering, Universitas
Mercu Buana, Indonesia

Email:

dian.widiastuti@mercubuana.ac.id

INTRODUCTION

Antennas with a low profile, a small size, and a wide bandwidth are highly sought after for a variety of applications due to the rapid growth of wireless systems such as Wi-Fi [1], 5G [2], etc. Substrate integrated waveguide (SIW) cavity antennas have received much attention in recent years because of their alluring benefits, including their affordability, simplicity of integration, and elevated radiation performance. Additionally, SIW cavity-backed antennas can be produced at a low-cost thanks to the ability to use the traditional

printed circuit board (PCB) process for the entire design. However, the thin substrate has a significant impact on the SIW cavity's quality factor, which results in a small operating bandwidth (BW) [3]. So, conventional SIW slot antennas are not the best option for multi-resonant achievement.

Researchers have suggested several methods to solve the limited-BW issue using slot antenna implementation into the planar SIW. By using two parallel slots of unequal length, an improvement in BW was achieved [4]. By using a

modified bow-tie coupling slot in the cavity layer for each 2 x 2 subarray antenna, the BW was improved [5]. A pair of bow-tie or hourglass-shaped slots can be used to enhance the impedance bandwidth without using additional complicated mechanisms that were recommended in [6]. The dumbbell slot, the half bow-tie complementary-ring slot, and shorting vias are used for creating the dual modes as presented by [7][8]. The shorting vias combined with a cross-shape slot or dual T-shape slot also can be used for bandwidth enhancement as presented by [9] and [10]. Integrating the modified spiral slot resonator (MSSR) with tilted slots and meta-surface loading resulted in triple resonance for bandwidth enhancement as presented by [11]. Bandwidth enhancement also can be achieved through aperture coupling that is formed by the feeding part [12]. The quality factor is extracted with characteristic mode analysis (CMA) between patch and shorting pins. It results in broadband impedance BW and stable elevated gain. Reference [13] used a combination of the hexagonal and rectangular slots to enhance bandwidth rather than use conventional slots. The aforementioned techniques are sufficient for enhancing BW by resulting in multi-resonant frequencies, however the full-mode SIW cavity technology results in larger antenna dimensions.

A theoretical approach for antenna miniaturization is provided in particular by fraction modes like half mode (HM-), quarter mode (QM-), and eighth mode (EM-) cavities. Despite having much smaller required sizes, they can still maintain a field spreading that resembles that of the full mode (FM). HM-, QM-, and EM-SIW cavities were used to miniaturize the conventional SIW slot antennas [14, 15, 16, 17, 18, 19, 20, 21, 22]. The electric field spreading for the dominant mode is the same in the HM-/QM-/EM-SIW cavities antennas. With the use of HMSIW and QMSIW cavities, the size of the antennas can be decreased to 50% and 25% while sustaining the same performance. The HMSIW cavity slot antennas stand out for their ability to meet the demands of wide impedance BW with small dimensions. There were few reports of HMSIW antennas with multi-resonant frequencies [23, 24, 25, 26, 27, 28]. The dual resonant frequencies have been reported by [23, 24, 25, 26, 26] by using rectangular slots, circular slots, triangular slots, and defective ground structures (DGS). The results have a broadband impedance BW by combining two adjacent resonant frequency modes. An HMSIW-based antenna with a wide-impedance BW also can be constructed by using cork material [27] and results in 1.3 GHz impedance BW. However,

because of the substrate's greater thickness, it can only be used on floors. Another HMSIW antenna with wideband BW has been presented in [28] by spending the epsilon-shaped slot to excite multi-resonant frequencies to merge. However, all BW of the presented reports are still below 30%. The suggested HMSIW antenna is an appealing choice to utilize in many real-world applications, particularly where the BW of the antenna is a main need, according to the results of the resonant mode analysis.

This paper presents an HMSIW antenna with a broadband BW in a single cavity for X-band application. The broadband BW is achieved by resulting multi-mode merge. The multi-mode merge itself is excited by using a demi-hexagonal ring slot shape. The measured BW enhances up to 34.46% (8.91 – 12.62 GHz) with more than triple frequencies resonant. The same demi-hexagonal ring slot is also used in reference [29] in the HMSIW structure. However, the previous reference has only one resonant with a restricted impedance bandwidth. It happens because of the differentiation cavity shape used and the feed line port location.

ANTENNA DESIGN

Antenna Evolution

The antenna design is presented in Figure 1a where it is similar to previous work presented in [26] and [30] in associations of HMSIW technology, but there are differences in the slot shape and HMSIW used. Unlike the prototypes from [26] and [30], which were intended to use dual HMSIW cavities among inner and outer, the recommended antenna design only used a single inner HMSIW cavity.

In comparison to FMSIW [31], the recommended antenna's HMSIW design provides a small dimension with a broadband impedance bandwidth. The suggested geometry is implemented on a one-layered RT/Duroid 5880 substrate using a loss tangent of 0.0009, a

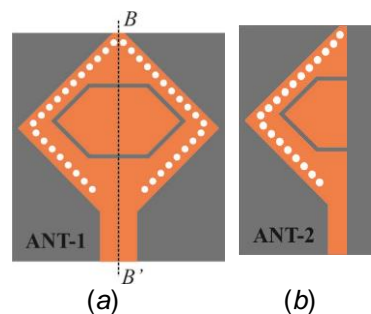


Figure 1. Antenna evolution: (a) FMSIW cavity with a hexagonal ring slot antenna, (b) HMSIW cavity using a demi-hexagonal ring slot antenna

dielectric constant of 2.2, and a depth of 1.57 mm. The metallic holes are arranged in a rectangular pattern near the cavity's side wall to create the half-rectangular SIW cavity. To reduce losses via the ideal electric conductor wall, the diameter holes (d) and space among the center of the hole (p) are specified following the SIW recommendations ($p/d \leq 2$ and $\lambda_0/d \geq 10$) [32, 33, 34].

The recommended antenna design is derived from the antenna's evolution, which is described in Figure 1. The recommended antenna design starts with the rectangular FMSIW cavity. The rectangular FMSIW cavity dimension is achieved by the frequency application into the antenna design where it can be calculated by (1) [35]. The hexagonal ring slot is added into the patch rectangular FMSIW cavity as displayed in Figure 1a (ANT-1).

The hexagonal ring slot is used for radiating an electric field into the air. The 260 MHz impedance bandwidth is resulted by ANT-1 that is on 11.85 – 12.11 GHz as shown in Figure 2. The low fractional bandwidth (2.17%) is achieved by ANT-1 because of only in single resonant frequency on TE₁₂₀ mode.

$$f_{mnp}^{SIW} = \frac{c}{2\pi\sqrt{\mu_r\epsilon_r}} \sqrt{\left(\frac{m\pi}{L_{eff}}\right)^2 + \left(\frac{n\pi}{h}\right)^2 + \left(\frac{p\pi}{W_{eff}}\right)^2} \quad (1)$$

By dividing symmetrically along BB' , a rectangular FMSIW cavity becomes two pieces of half-rectangular cavities as shown in Figure 1b. The half-rectangular cavity with a demi-hexagonal ring slot shape is achieved as called ANT-2. The ANT-2 has 2990 MHz impedance bandwidth as displayed in Figure 2. The ANT-2 resonance on 9.65 – 12.64 GHz. The broadband impedance bandwidth is achieved on ANT-2

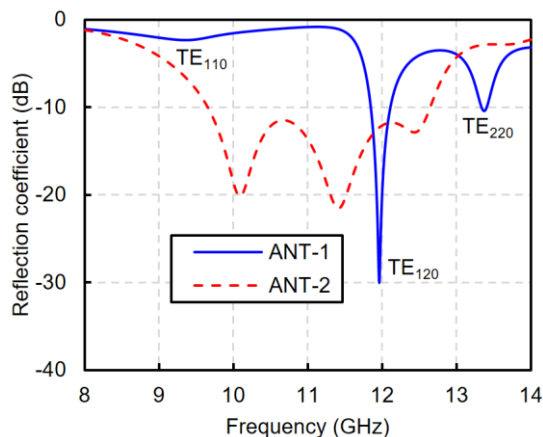


Figure 2. Coefficient reflection simulation for antenna evolution

because of a higher fractional bandwidth (26.83%) than the ANT-1. The final of the recommended antenna design (ANT-2) dimension is displayed in Figure 3, while the dimension of the ANT-2 is tabularized in Table 1. The recommended antenna design is created by spending Ansys HFSS electromagnetic simulator.

Electric Field

The recommended antenna design has a broadband impedance bandwidth by developing in triple frequencies resonant. The triple frequencies resonant consists of several adjacent TE modes joined together for a wider impedance bandwidth. The adjacent TE modes consist of TE₁₁₀, TE₁₂₀, TE₂₂₀, and TE₁₃₀ mode combinations that are analyzed by electric field spreading as shown in Figure 4, Figure 5, and Figure 6.

Figure 4 shows the first resonance that occurs at 10.1 GHz. The electric field spreading at 10.1 GHz takes place because of a blend of TE₁₁₀ and TE₁₂₀ modes. The stronger TE₁₂₀ mode happens than the TE₁₁₀ mode. It can be seen in the differentiation phase between up and down slot segments. The electric field spreading in the second resonant occurs on the 11.42 GHz as shown in Figure 5. It shows the electric field spreading combination between odd and even TE₂₂₀ modes.

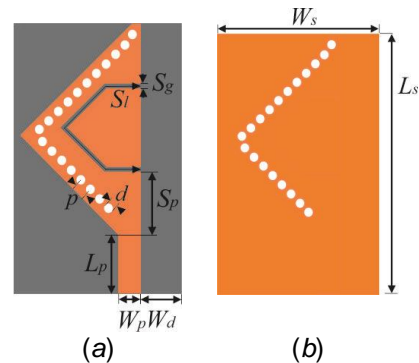


Figure 3. The geometric of the ANT-2 dimension: (a) top layer. (b) ground layer

Parameter	Dimension (mm)	Description
W_s	18.5	substrate width
L_s	30	substrate length
d	1	diameter vias
p	1.5	distance between two vias center
W_p	2.425	port width
L_p	6.5	port length
W_d	4.5	gap width
S_p	7	slot position
S_g	0.6	slot gap
S_i	20.90	slot length

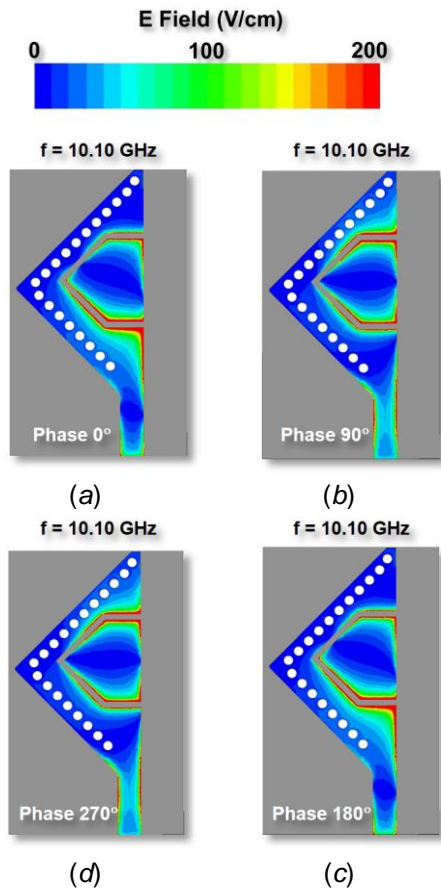


Figure 4. The electric field distribution on 10.10 GHz at phase: (a) 0°, (b) 90°, (c) 180°, and (d) 270°

It can be analyzed by the same electric field spreading between the up, down, and right slot segments. They alternate every 90° steps.

The third resonant electric field spreading at 12.45 GHz is depicted in Figure 6. It displays the combination of the electric field spreading between the TE₁₃₀ and TE₂₂₀ modes in the same phases. The same electric field spreading between the up, down, and right slot segments can be utilized for investigating it. Every 90° steps, they switch places.

Dual Polarization

The recommended antenna design has dual polarization i.e. linear and circular polarization as shown in Figure 7. Circular polarization emerges when the two orthogonal electric field component vectors have equal magnitudes and are identically 90°, or one-quarter wavelength, out of phase. Circular polarization can occur in this recommended antenna design because the hexagonal slot is almost the same as the circle slot while the 90°

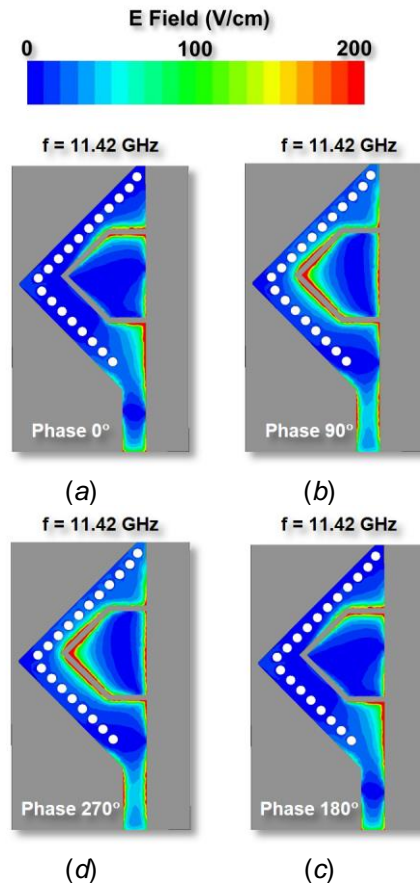


Figure 5. The electric field distribution on 11.42 GHz at phase: (a) 0°, (b) 90°, (c) 180°, and (d) 270°

phase differentiation is generated by TE₁₂₀ or TE₂₂₀ modes.

The recommended antenna design (ANT-2) has circular polarization even right-handed circular polarization (RHCP) or left-handed circular polarization (LHCP) on 10.23 – 10.58 GHz (350 MHz) with a 3.36% axial ratio percentage. The recommended LHCP antenna design is achieved by mirroring the RHCP antenna dimension.

Parametric Investigation

The impedance bandwidth enhancement is predisposed by the slot length (S_l), the slot gap (S_g), and the slot position (S_p) as shown in Figure 8, Figure 9, and Figure 10. The triple frequency resonance disappears when the slot length is less than one guided wavelength for TE₁₁₀ mode (9 GHz) as shown in Figure 8. The first and the third resonant frequencies shift into the lower frequency. A broadband bandwidth with triple frequencies resonant disappears and becomes a dual-band impedance bandwidth.

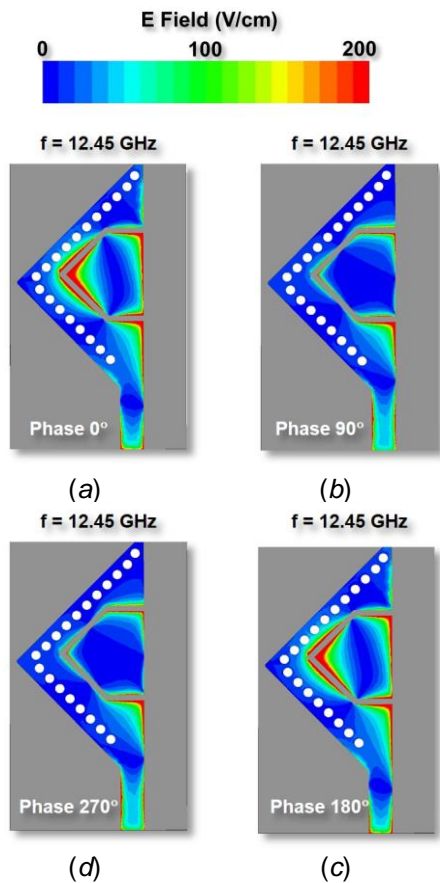


Figure 6. The electric field distribution on 12.45 GHz at phase: (a) 0°, (b) 90°, (c) 180°, and (d) 270°

Figure 9 shows the parametric investigations for the slot gap variations. A thin slot gap causes the broadband impedance bandwidth to disappear and shift to lower frequencies. The broadband impedance bandwidth occurs on a 0.6 mm slot gap value with 26.95% (9.63-12.62 GHz) fractional bandwidth.

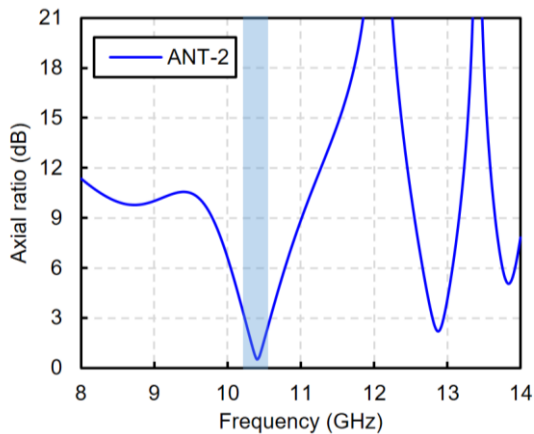


Figure 7. The ANT-2 axial ratio simulation

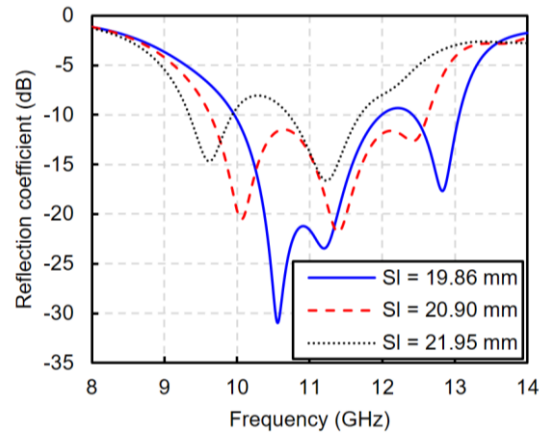


Figure 8. The parametric studies for the slot length variations

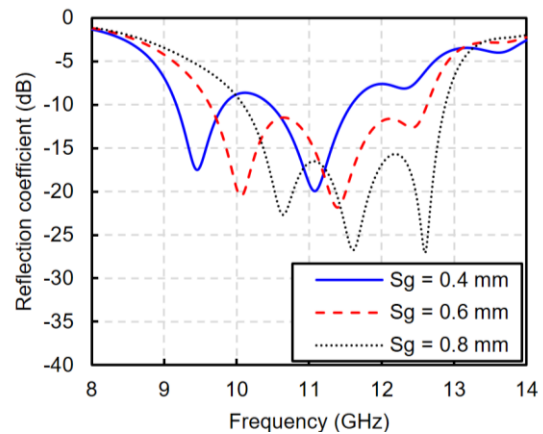


Figure 9. The parametric studies for the slot gap variations

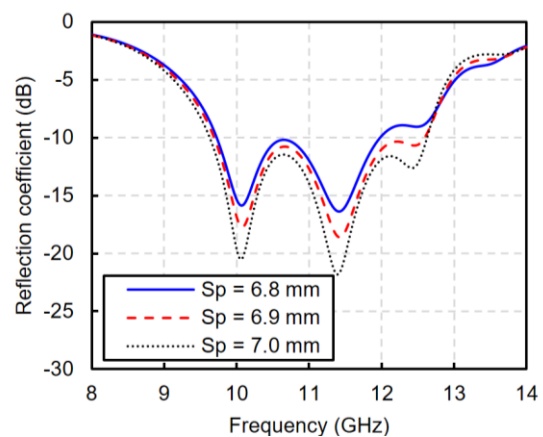


Figure 10. The parametric studies for the slot position variations

The impedance bandwidth antenna becomes larger as shifts into the upper side rectangular cavity as shown in Figure 10. It occurs because of the third resonant joint with the first and the second resonant. The optimization of this antenna design was achieved at 7.0 mm for the slot position.

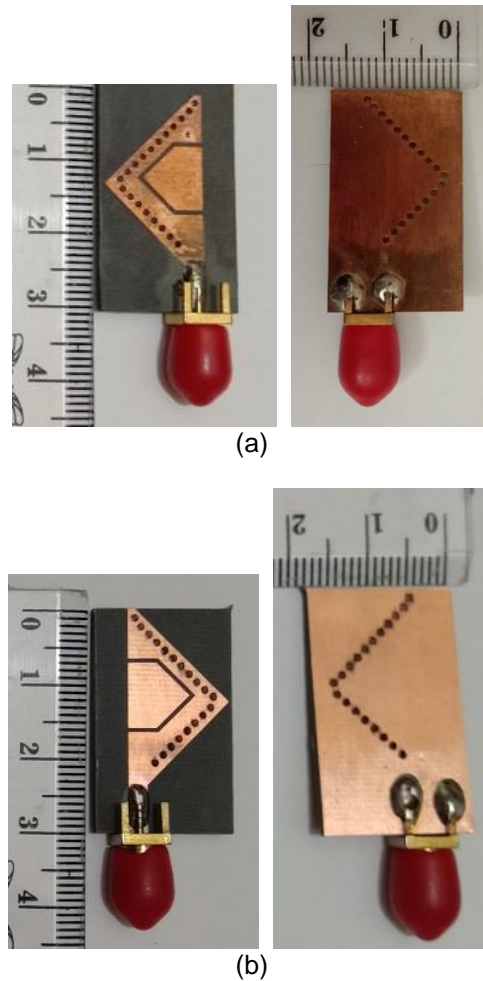


Figure 11. Antenna fabrication for (a) RHCP and (b) LHCP

RESULTS AND DISCUSSION

Antenna Fabrication

The recommended antenna design is manufactured by utilizing photo etching on the Duroid/RO 5880 with 1.575 mm substrate thickness. The manufacture of the recommended antenna design (ANT-2) is displayed in Figure 11. Figure 11a shows the manufacture of the RHCP while the opposite of RHCP is shown in Figure 11b as the LHCP one. The demi-hexagon ring slot shape is scratched on the top layer while the ground layer is full of copper layers.

Measurement

The recommended antenna design is measured by using a Vector Network Analyzer for measuring impedance bandwidth. The 3.33 GHz (9.35 – 12.68 GHz) impedance bandwidth measured is achieved for the RHCP antenna design (ANT-2), while the impedance bandwidth simulated of the RHCP antenna design is 2.99 GHz (9.65 – 12.64 GHz).

The impedance bandwidth measured is wider than the impedance bandwidth simulated as displayed in Figure 12.

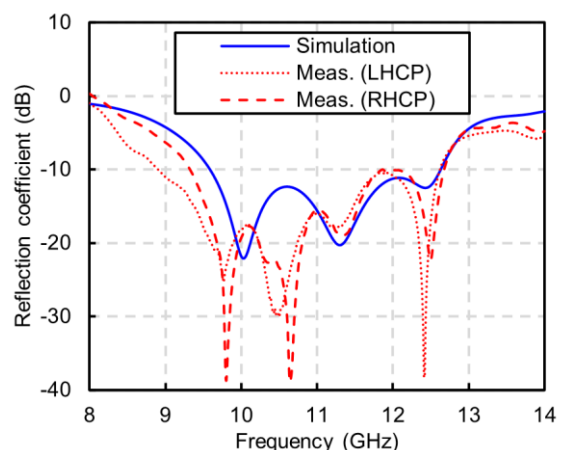


Figure 12. The ANT-2 reflection coefficient comparison among simulation and measurement for RHCP, and LHCP

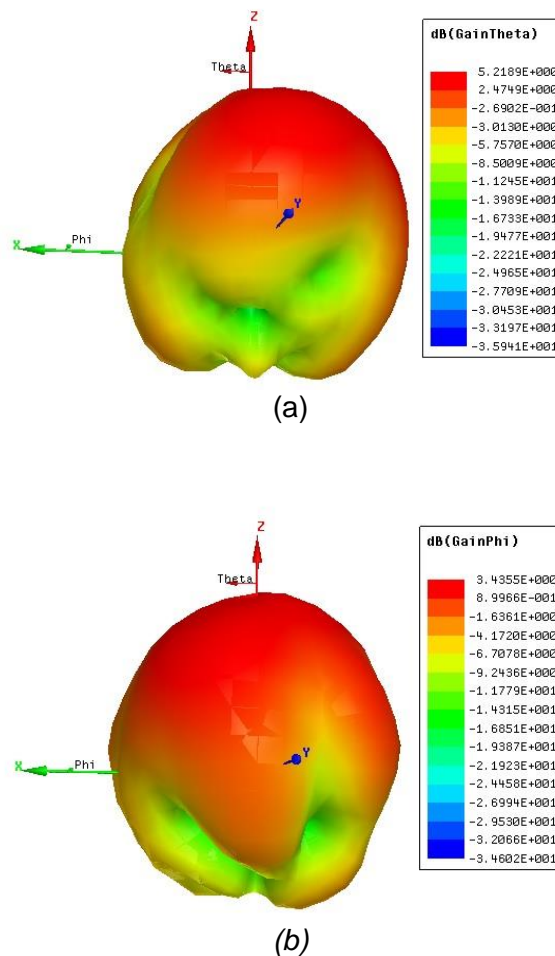


Figure 13. The radiation pattern simulation on 10.45 GHz for (a) E-plane and (b) H-plane.

Table 2. Comparison of the recommended antenna result with the previous research in the HMSIW structure

Ref.	Substrate type	Substrate thickness (mm)	Substrate dimension (λ_0^2)	BW (GHz)	Fc (GHz)	FBW (%)
[23]	RO 5880	0.78	0.48×0.24	0.5	8.64	5.67
[24]	RO 5880	0.508	0.65×0.26	3.53	27.5	12.84
[27]	Cork Material	3	0.64×0.64	1.3	5.5	23.64
[28]	RO 5880	1.575	0.87×0.6	0.73	5.45	13.29
[25]	RO 5880	1.575	0.4×0.4	0.38	3.85	9.87
[26]	RO 5880	1.575	0.72×0.37	0.88	6.15	14.31
[30]	RO 5880	1.575	1.63×0.67	3.46	10.87	31.83
This Work (RHCP)	RO-5880	1.575	1.08×0.66	3.33	11.02	30.23
This Work (LHCP)	RO-5880	1.575	1.08×0.66	3.71	10.77	34.46

The same condition also occurs with the LHCP antenna design. The 34.46% (8.91 – 12.62 GHz) of fractional bandwidth measured is achieved for the LHCP antenna design. The quad- and penta-resonance are achieved in the reflection coefficient measured. The difference in the number of resonances and the width of the

impedance bandwidth between the simulated and measured reflection coefficients are most likely caused by imperfections in the vias walls in the antenna fabrication.

The radiation pattern simulation is displayed in Figure 13 for E-plane and H-plane at 10.45 GHz. The E-plane has a higher gain rather

than the H-plane. The E-plane has a 5.22 dBi gain while the H-plane has a 3.44 dBi gain. The E-plane and H-plane have an omnidirectional antenna direction. The comparison of the recommended antenna result with the previous research is listed in [Table 2](#).

CONCLUSION

The broadband bandwidth antenna is reported in this paper by resulting in triple frequencies resonant for solving a narrow impedance bandwidth. The 30.23% (9.35 - 12.68 GHz) fractional bandwidth is measured for the right-handed circular polarization (RHCP) antenna while the left-handed circular polarization (LHCP) antenna has a 34.46% (8.91–12.62 GHz) fractional bandwidth. The measurement results are in good agreement with the simulation results. Each antenna has 50% miniaturization because of using a single HMSIW structure rather than previous research. The antenna can be applied to the X-band application (8 - 12 GHz).

ACKNOWLEDGMENT

This research was supported/partially supported by Universitas Mercu Buana, Kerjasama Luar Negeri number 02-5/702/B-SPK/V/2023. In addition, we thank our colleagues from Huda A Majid who provided insight and expertise that greatly assisted this research.

REFERENCES

- [1] D. Rusdiyanto, C. Apriono, D. W. Astuti, and M. Muslim, "Bandwidth and Gain Enhancement of Microstrip Antenna Using Defected Ground Structure and Horizontal Patch Gap," *SINERGI*, vol. 25, no. 2, p. 153, 2021, doi: 10.22441/sinergi.2021.2.006
- [2] Y. Rahayu, Y. B. Pradana, and Y. Yamada, "Dual-band frequency reconfigurable 5G microstrip antenna," *SINERGI*, vol. 27, no. 1, pp. 81–88, 2023, doi: 10.22441/sinergi.2023.1.010
- [3] A. K. Pandey, N. K. Sahu, R. K. Gangwar, and R. K. Chaudhary, "A SIW-Cavity-Backed Wideband Circularly Polarized Antenna Using Modified Split-Ring Slot as a Radiator for mm-Wave IoT Applications," *IEEE Internet of Things Journal*, vol. 11, no. 7, pp. 11793–11799, 2023, doi: 10.1109/JIOT.2023.3332169
- [4] R. Zhao, B. Liu, Y. Ma, W. Xing, and X. Sun, "Design of a substrate-integrated waveguide based slot-pair array antenna for bandwidth enhancement," *IET Microwaves, Antennas Propagation*, vol. 14, no. 13, pp. 1481–1487, 2020, doi: 10.1049/iet-map.2019.0307
- [5] W. Y. Yong, A. Haddadi, T. Emanuelsson, and A. A. Glazunov, "A Bandwidth-Enhanced Cavity-Backed Slot Array Antenna for mmWave Fixed-Beam Applications," *IEEE Antennas and Wireless Propagation Letters*, vol. 19, no. 11, pp. 1924–1928, 2020, doi: 10.1109/LAWP.2020.3022988
- [6] A. Desai, Y. T. Hsu, and H. Heng-tung, "High gain substrate integrated waveguide antenna with enhanced bandwidth for millimeter-wave wireless network applications," *Wireless Networks*, vol. 29, no. 5, pp. 2251–2260, 2023, doi: 10.1007/s11276-023-03296-7
- [7] D. W. Astuti, S. A. Togatorop, M. Muslim, and Y. Natali, "Peningkatan Persentase Lebar Pita Antena 5G Substrate Integrated Waveguide dengan Slot Dumbbell," *ELKOMIKA: Jurnal Teknik Energi Elektrik, Teknik Telekomunikasi, & Teknik Elektronika*, vol. 12, no. 3, p. 597, 2024, doi: 10.26760/elkomika.v12i3.597
- [8] S. M. Patil and R. Venkatesan, "Bandwidth enhancement of substrate integrated waveguide cavity-backed half bow-tie complementary-ring slot antenna for Ku-band applications," *Alexandria Engineering Journal*, vol. 81, no. September, pp. 46–54, 2023, doi: 10.1016/j.aej.2023.08.082
- [9] L. Xiang, Y. Zhang, Y. Yu, and W. Hong, "Characterization and Design of Wideband Penta- And Hepta-Resonance SIW Elliptical Cavity-Backed Slot Antennas," *IEEE Access*, vol. 8, pp. 111987–111994, 2020, doi: 10.1109/ACCESS.2020.3002433
- [10] D. Chaturvedi, A. A. Althwayb, and A. Kumar, "Bandwidth enhancement of a planar SIW cavity - backed slot antenna using slot and metallic - shorting via," *Applied Physics A*, vol. 128, no. 3, pp. 1–7, 2022, doi: 10.1007/s00339-022-05309-2
- [11] A. Gorai, A. Deb, J. R. Panda, and R. Ghatak, "Millimeter Wave/5G Multiband SIW Antenna with Metasurface Loading for Circular Polarization and Bandwidth Enhancement," *Journal of Infrared, Millimeter, and Terahertz Waves*, vol. 43, no. 5, pp. 366–383, 2022, doi: 10.1007/s10762-022-00858-2
- [12] X. Zhang, T. Tan, Q. Wu, L. Zhu, S. Zhong, and T. Yuan, "Pin-Loaded Patch Antenna Fed With a Dual-Mode SIW Resonator for Bandwidth Enhancement and Stable High Gain," *IEEE Antennas and Wireless Propagation Letters*, vol. 20, no. 2, pp. 279–283, 2021, doi: 10.1109/LAWP.2020.3048749

- [13] E. Vinodha, "A broadband low profile SIW cavity-backed antenna loaded with hexagonal and rectangular slots for ' X ' band application," *Analog Integrated Circuits and Signal Processing.*, vol. 118, no. 2, pp. 307–315, 2024, doi: 10.1007/s10470-023-02238-9
- [14] S. Banerjee, S. Das Mazumdar, S. Chatterjee, and S. K. Parui, "Half mode semi-hexagonal SIW antennas and arrays for cellular V2X communication," *Microsystem Technologies*, vol. 27, no. 10, pp. 3639–3651, 2021, doi: 10.1007/s00542-020-05127-7
- [15] B. Pramodini and D. Chaturvedi, "Miniaturized Inverted L-Shaped Slot Antenna Using HMSIW Technology," in *2023 2nd International Conference on Paradigm Shifts in Communications Embedded Systems, Machine Learning and Signal Processing, PCEMS 2023*, 2023, pp. 1–4, doi: 10.1109/PCEMS58491.2023.10136069
- [16] X. Guan, Z. Xue, W. Ren, and W. Li, "Single-Layer Circular Polarized Endfire Antenna Based on HMSIW and Quasi-Yagi," in *Proceedings - 2023 Cross Strait Radio Science and Wireless Technology Conference, CSRSWTC 2023*, 2023, pp. 1–3, doi: 10.1109/CSRSWTC60855.2023.10427133
- [17] R. K. Barik, S. Koziel, Q. S. Cheng, and S. Szczepanski, "Highly Miniaturized Self-Diplexed U-Shaped Slot Antenna Based on Shielded QMSIW," *IEEE Access*, vol. 9, pp. 158926–158935, 2021, doi: 10.1109/ACCESS.2021.3131174
- [18] Y. X. Sun and D. Wu, "QMSIW Cavities for Compact Dual-Frequency Millimeter-Wave 5G Antenna Array Design," in *2021 International Symposium on Antennas and Propagation, ISAP 2021*, 2021, pp. 5–6, doi: 10.23919/ISAP47258.2021.9614558
- [19] M. Lai and Y. D. Kong, "A Low-Profile High-Gain Circularly Polarized Antenna Using Quarter-Mode Substrate Integrated Waveguide Technique," in *2021 International Conference on Microwave and Millimeter Wave Technology, ICMMT 2021 - Proceedings*, 2021, pp. 1–3, doi: 10.1109/ICMMT52847.2021.9618488
- [20] V. Jaya Prakash and D. S. Chandu, "Compact Four-Element Quarter Mode Circular SIW Based MIMO Antenna with Enhanced Isolation," *Wireless Personal Communications.*, vol. 133, no. 1, pp. 625–640, 2023, doi: 10.1007/s11277-023-10783-9
- [21] D. Chaturvedi and A. Kumar, "A QMSIW Cavity-Backed Self-Diplexing Antenna With Tunable Resonant Frequency Using CSRR Slot," *IEEE Antennas and Wireless Propagation Letters*, vol. 23, no. 1, pp. 259–263, 2024.
- [22] J. Zhou and M. Yang, "A Low-Profile Eighth-Mode SIW Antenna With Dual-Sense Circular Polarization, Enhanced Bandwidth and Simple Structure," in *IEEE Access*, vol. 9, pp. 144375–144384, 2021, doi: 10.1109/ACCESS.2021.3122028
- [23] S. A. Razavi and M. H. Neshati, "Development of a Low-Profile Circularly Polarized Cavity-Backed Antenna Using HMSIW Technique," *IEEE Transactions on Antennas and Propagation*, vol. 61, no. 3, pp. 1041–1047, 2013, doi: 10.1109/TAP.2012.2227104
- [24] Q. Wu, H. Wang, C. Yu, and W. Hong, "Low-Profile Circularly Polarized Cavity-Backed Antennas Using SIW Techniques," *IEEE Transactions on Antennas and Propagation.*, vol. 64, no. 7, pp. 2832–2839, 2016, doi: 10.1109/TAP.2016.2560940
- [25] D. W. Astuti, M. Asvial, F. Y. Zulkifli, and E. T. Rahardjo, "Bandwidth Enhancement on Half-Mode Substrate Integrated Waveguide Antenna Using Cavity-Backed Triangular Slot," *International Journal of Antennas and Propagation*, vol. 2020, 2020, doi: 10.1155/2020/1212894
- [26] D. W. Astuti *et al.*, "Bandwidth Enhancement for Half Mode Substrate Integrated Waveguide Antenna using Defected Ground Structures," *International Journal of Electronics and Telecommunication*, vol. 69, no. 3, pp. 449–454, 2023, doi: 10.24425/ijet.2023.144382
- [27] O. Caytan *et al.*, "Half-Mode Substrate-Integrated-Waveguide Cavity-Backed Slot Antenna on Cork Substrate," *IEEE Antennas and Wireless Propagation Letters*, vol. 15, pp. 162–165, 2016, doi: 10.1109/LAWP.2015.2435891
- [28] D. Chaturvedi, A. Kumar, and S. Raghavan, "Wideband HMSIW-Based Slotted Antenna for Wireless Fidelity Application," *IET Microwaves, Antennas & Propagation*, vol. 13, no. 2, pp. 258–262, 2019, doi: 10.1049/iet-map.2018.5110
- [29] D. Chaturvedi and S. Raghavan, "A Half-Mode SIW Cavity-Backed Semi-Hexagonal Slot Antenna for WBAN Application," *IETE Journal of Research*, pp. 1–7, Apr. 2018, doi: 10.1080/03772063.2018.1452644
- [30] D. W. Astuti, Y. Wahyu, F. Y. Zulkifli, and E. T. Rahardjo, "Hybrid HMSIW Cavity Antenna

- with a Half Pentagon Ring Slot for Bandwidth Enhancement," *IEEE Access*, vol. 11, no. February, pp. 18417–18426, 2023.
- [31] S. Sepryanto, S. Attamimi, and F. Sirait, "Perancangan Antena Mikrostrip SIW Cavity-Backed Modified Dumbell-Shaped Slot Untuk Pengaplikasian Pada 5G," *Jurnal Teknologi Elektro*, vol. 11, no. 2, pp. 115–119, 2020, doi: 10.22441/jte.2020.v11i2.008
- [32] E. Aparna, G. Ram, and G. A. Kumar, "Review on Substrate Integrated Waveguide Cavity Backed Slot Antennas," *IEEE Access*, vol. 10, no. November, pp. 133504–133525, 2022, doi: 10.1109/ACCESS.2022.3231984
- [33] M. Darsono and M. Rega, "Optimization of Ultra-Wideband bandwidth for the design of microstrip monopole antennas using Defected Ground Structure and star-shaped patches," *SINERGI*, vol. 27, no. 3, pp. 309-318, 2023, doi: 10.22441/sinergi.2023.3.002
- [34] A. Firdausi, L. Damayanti, G. P. N. Hakim, U. Umaisaroh, M. Alaydrus, "Design of A Dual-Band Microstrip Antenna for 5G Communication," *Journal of Integrated and Advanced Engineering (JIAE)*, vol. 1, no. 1, pp. 65-72, 2021, doi: 10.51662/jiae.v1i1.15
- [34] D. M. Pozar, *Microwave engineering*, 4th ed. John Wiley & Son, Inc, 2012.